

## Observation of Density Fluctuations during Crystallization

Klaus Schätzel<sup>(a)</sup> and Bruce J. Ackerson

*Department of Physics, Oklahoma State University, Stillwater, Oklahoma 74078*

(Received 28 May 1991)

Long-wavelength density fluctuations are monitored by small-angle light scattering during the crystallization of hard colloidal spheres. These measurements demonstrate the coupling of the density, a conserved parameter, to the previously measured nonconserved crystal order parameter.

PACS numbers: 64.70.Dv, 81.10.Fq, 82.70.Dd

Crystallization, the disorder-to-order transition from fluids to solids, constitutes a first-order phase transition which is typically governed by the nonlinear coupling of several parameters like density, energy, and the crystal order parameter. The complexity introduced by these couplings has limited theoretical progress largely to the study of simpler systems [1] or to purely phenomenological approaches [2]. Experimentally there is a paucity of data on crystallization kinetics, which may be due to the typically rapid progress of homogeneous nucleation in atomic systems and practical difficulties in preventing the dominance of heterogeneous nucleation. However, recent work on polymers [3] and colloids [4] has demonstrated systems which allow convenient real-time observation of phenomena like homogeneous nucleation and crystal growth.

Early work on colloidal crystals focused on phase behavior [5–7] and static structure of the solid phase(s) [8–13]. Subsequent first studies of crystallization kinetics in colloids include direct microscopic observations [14], turbidity measurements [15], and a few time-resolved measurements of crystal-peak amplitudes in the static structure factor [9]. These limited data appear to be in rough agreement with classical phenomenological theories of nucleation and growth [16].

All of the cited measurements focused on the crystal order parameter, a nonconserved quantity, having a value of zero in the initial supersaturated amorphous state and some finite value in the (poly)crystal state. This order parameter is coupled, in general, to a second important conserved parameter, the local density of colloidal particles. Unlike in atomic systems, no further parameters are conserved, since particle energy and momentum are shared with the solvent. In this Letter we present the first direct measurements of density fluctuations during the crystallization of colloids, which illuminate the importance of both parameters, their coupling, and may lead to new insight into the crystallization process.

As our samples we used polymeric spherical particles consisting of a polymethylmethacrylate core coated by a thin layer of hydroxystearic acid in order to prevent flocculation [17]. These particles were refractive-index matched in a suitable mixture of decalin and tetralin to produce clear samples with little multiple scattering of visible light. As evidenced by phase behavior [5,18], sedi-

mentation properties [18], their reactions to steady and oscillatory shear [19], and electrophoretic mobility measurements [20], these colloidal particles show very little long-range interactions and closely approximate ideal hard spheres. We chose a particle diameter of 1  $\mu\text{m}$ , for which crystallization appears to start homogeneously throughout the sample with little tendency to grow heterogeneous crystals on the cell walls. As mean particle density (rather than temperature) is used as the control parameter, samples were prepared at several densities in the coexistence region and at higher densities up to the glass transition. Phase separation under the action of gravity was sufficiently slow [18] that it did not interfere with most of our measurements.

Samples at equilibrium demonstrated polycrystalline behavior with the first-order Debye-Scherrer powder pattern ring occurring at  $q \approx 10^4/\text{mm}$ . These crystals may be shear melted [21] by a sufficiently large shear stress and are found to be in a metastable amorphous state [22] upon cessation of the shear flow. For purposes of comparing experimental results with existing theory, it is assumed that this “shear melted” state is equivalent to a density quench from a low-density fluid state. Samples were stirred and tumbled in order to assure complete shear melting, which was monitored in large-angle light scattering, and then were left to crystallize. The crystallization process was observed in small-angle light scattering produced by illumination of the sample with an expanded, spatially filtered laser beam (HeNe laser, 5 mW, polarized) focused to a distant screen. A charge-coupled-device camera recorded the scattered intensity distributions. These data were digitized, stored, and evaluated on a personal computer. Data recording sequences ran from a few hours to a few days. Data processing involved background subtraction—typically using an early image of a sequence—and angular averaging yielding unnormalized structure factor data  $s(q)$ , where the scattering vector  $q$  typically varied from 10/mm to  $10^3/\text{mm}$ .

Previous structure-factor measurements of order-disorder transitions typically focused on one nonconserved order parameter, which then shows a monotonic decay of the structure factor with  $q$ , often satisfying a simple scaling law [1,23]. In contrast to these studies, the most prominent feature of our measurements was a marked peak in the structure factor at finite  $q > 0$ , easily observ-

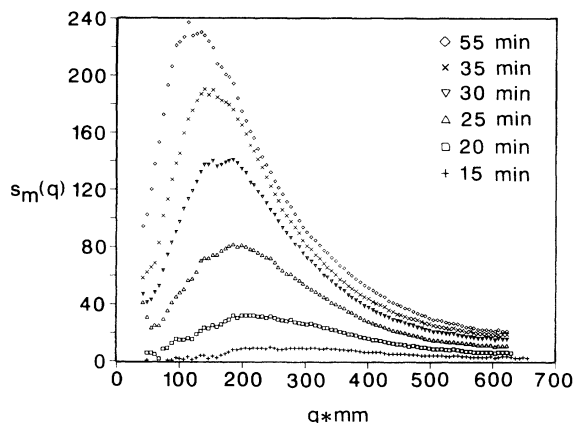


FIG. 1. Intensity distribution  $s(q)$  vs scattered wave vector  $q$  and parametrized by the time after shear melting.

able on all samples around the melting density. The vanishing of the scattered intensity  $s(q)$  towards zero wave vectors is an immediate consequence of the conservation of particle density, the fluctuations of which produce the observed low angle scattering. In this Letter we present data only for a volume fraction of 0.54 corresponding to 95% crystal phase in equilibrium (Fig. 1).

Peak intensities generally rise with time and peak positions move to smaller  $q$  values, indicating crystal growth (Fig. 1). Qualitatively, this behavior is similar to that observed for spinodal decomposition phenomena [1,24], but there are considerable quantitative deviations in the scattered intensity wave vector and time dependences. For each measurement of  $s(q)$ , we determined the peak intensity  $s_m$  and as a measure of a characteristic wave vector,  $q_{1/2}$ , the larger  $q$  value where  $s(q)$  falls to  $\frac{1}{2}$  of its maximum. The resulting data are shown in Fig. 2 and clearly reveal the existence of two distinct time regimes. At small times, we observe a “fast process” with a rapid growth of the peak intensity accompanied by some decrease in the characteristic wave vector. Separated by an intermediate “crossover” phase with little change in either peak height or position, there follows a second “slow process.” The latter is characterized by a moderate growth in peak intensity and a shift of the peak towards smaller values of  $q$ .

If the  $s(q)$  data are rescaled by using peak intensity  $s_m$  and characteristic wave vector  $q_{1/2}$  as units of  $s$  and  $q$ , approximate scaling is observed to hold throughout both the “fast” and “slow” processes, with some deviation in the crossover phase. A suitable empirical fitting function to the scaled radial intensity data is

$$S(Q) = s(q)/s_m = 27Q^2/2(1 + 2Q^2)^3, \quad (1)$$

with  $Q = q/q_{1/2}$ , as demonstrated in Fig. 3. Note that this function provides a significantly better fit to our data than Furukawa’s prediction for spinodal decomposition

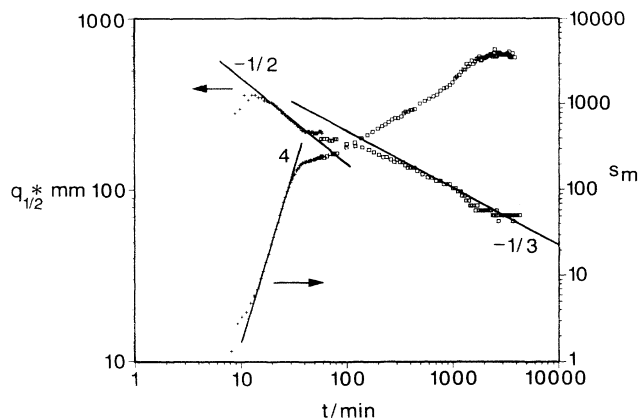


FIG. 2. The right abscissa corresponds to the maximum  $s_m$  in the intensity distribution while the left gives the characteristic wave vector  $q_{1/2}$  as a function of time after shear melting. The symbols + and  $\square$  correspond to separate experimental runs primarily in the small and large time regimes, respectively.

[25],

$$S(Q) = 3Q'^2/(2 + Q'^6), \quad (2)$$

with  $Q' = 1.504Q$ . Finally, we checked the scaling prediction of a peak height which should vary like the third power of a typical length scale, e.g., the inverse of our characteristic wave vector [1,25]. Figure 4 verifies such a scaling behavior for our slow process. For the fast process a more dramatic rise of intensity with spatial scale is observed.

These data may be interpreted in terms of the Avrami [26] picture of the crystallization process. Initially, we observe the nucleation of crystals accompanied by some

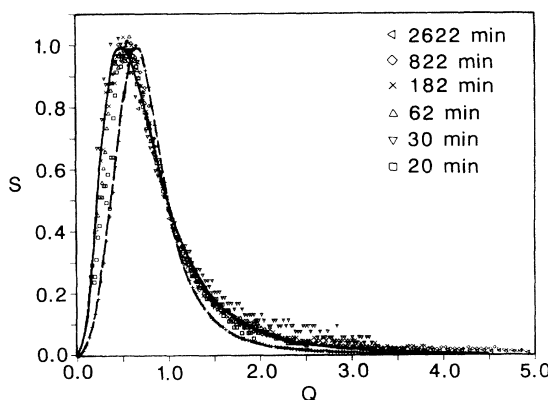


FIG. 3. Scaling of the intensity distribution including times in the “fast” (20 min, 30 min), crossover (62 min), and “slow” processes (182 min, 822 min, 2622 min). The greatest deviations from the empirical fitting function of Eq. (1) (continuous line) are produced in the crossover region. The Furukawa prediction for spinodal decomposition is shown as a broken line for comparison.

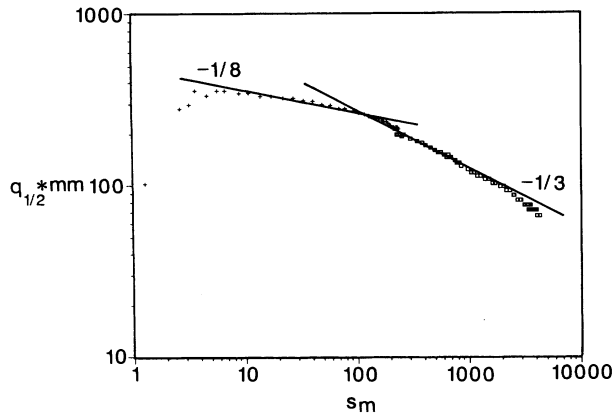


FIG. 4. The discussed scaling relations between peak amplitude  $s_m$  and characteristic wave vector  $q_{1/2}$  are apparent by approximate slopes of  $-1/8$  at early and  $-1/3$  at late times. The symbols  $+$  and  $\times$  correspond to separate experimental runs primarily in the small and large time regimes, respectively.

growth. Assuming for simplicity a constant nucleation rate and a self-similar density profile of the growing crystals at early times, we would expect a growth of the peak intensity  $s_m$  like  $t^{6m+1}$ , if  $t$  denoted time and the crystal diameter grew like  $t^m$ . All our measured data, however, certainly deviate from the expected linear crystal growth [16,27] with  $m=1$ . Instead both intensity and characteristic wave-vector data are well described if we assume a square root of time growth law with  $m=1/2$ . This assumption leads to the  $t^4$  rise in peak intensity as well as the  $t^{-1/2}$  shrinking in the characteristic wave vector which are both indicated in Fig. 2.

The measured characteristic wave vector for times less than about 10 min is subject to large error because the scattered intensity is very weak (see Fig. 1). We do not attribute any significance to the apparent increase in the characteristic wave vector for these times. The initial nucleation and growth phase stops when the crystallites fill most of the sample volume, leaving neither nucleation sites nor space for further growth. This crossover regime, which may be associated with percolation of the crystallized phase, is characterized by rather strong fluctuations in our scattering data between subsequent runs. Some measurements performed at different locations in the sample also indicate a systematic height dependence during crossover, which would imply a surprisingly rapid response of the system to gravity. Also in the crossover regime the sample transforms gradually from isolated crystallites embedded in a characteristic depletion zone to an almost close-packed polycrystalline arrangement, where density changes—and hence small-angle light scattering—are essentially slaved to grain boundaries.

The behavior at large times, the slow process, is compatible with ripening, where the growth of crystallites occurs at the expense of a reduction of their number. As-

suming a constant total crystal volume, the number of crystallites must decrease with the third power of inverse crystal diameter. If each crystal scatters at a peak intensity growing like the sixth power of diameter, we obtain a scaling of peak intensity like the third power of crystal size, which agrees with our data in Fig. 4. The value of the growth exponent as a function of time determined from the characteristic wave vector (see Fig. 2) is close to  $1/3$  for this sample which has a concentration slightly less than the melting value. Such an exponent corresponds to the Lifshitz-Slyozov theory for transitions with a conserved order parameter [1,28] with phase separation into high- and low-density phases. For more concentrated samples which are fully crystalline in equilibrium, the same intensity-size scaling holds but the temporal growth exponent of the characteristic wave vector is close to  $1/2$ . This exponent corresponds to the value predicted by the Lifshitz-Allen-Cahn growth law [1,29] for transitions dominated by a nonconserved order parameter [30]. The density fluctuations may have become slaved to the nonconserved order parameter in this case, since concentration variations will be primarily at the grain boundaries. In the former case with coexisting equilibrium phases and a  $1/3$  exponent, there is still equilibration between liquid and crystal phases and the density may not become slaved to the nonconserved order parameter.

A more fundamental picture of the crystallization phase transition should be built upon the explicit assumption of two relevant parameters, the crystal order parameter and the density. The free-energy functional depends upon both parameters, hence they are coupled, typically in a nonlinear fashion. Linearization of the equations of motion resulting from such an approach about the initial amorphous state can indeed be shown to lead to finite wavelength instabilities in the density, which are driven by a spontaneous decay of the system towards increasing crystalline order [31]. We will pursue further work on this approach in the future.

In conclusion, time-resolved measurements of small-angle light scattering by colloids during crystallization show a peak at finite wave vectors. Peak position and intensity may be used to determine the sizes of crystallites and their growth behavior. An initial nucleation-growth regime can be clearly separated from a late-stage ripening. Scaling of the structure factor seems to hold at all times except for the crossover region between the two growth regimes, where the crystallized phase first percolates the sample. The detailed information available in low angle scattering, like absolute determination of the size of crystallites as a function of time, proves the close coupling of the two parameters, the density and the crystal order parameter.

The authors thank David Cannell and Noel Clark for useful discussions, the Department of Energy for support through Grant No. DE-FG05-88ER45349 to B.J.A., and the Deutsche Forschungsgemeinschaft for a Heisenberg fellowship awarded to K.S.

- <sup>(a)</sup>On leave from Institut für Angewandte Physik, Universität D-2300 Kiel, Germany.
- [1] J. D. Gunton, M. San Miguel, and P. S. Sahni, in *Phase Transitions and Critical Phenomena*, edited by C. Domb and L. Lebowitz (Academic, New York, 1983), Vol. 8, p. 269.
- [2] J. Frenkel, *Kinetic Theory of Liquids* (Dover, New York, 1946).
- [3] C. R. Harkless, M. A. Singh, S. E. Nagler, G. B. Stephenson, and J. L. Jordan-Sweet, *Phys. Rev. Lett.* **64**, 2285 (1990).
- [4] *Phase Transitions in Colloidal Suspensions*, edited by B. J. Ackerson [Phase Transitions **21** (1990)].
- [5] P. N. Pusey and W. van Meegen, *Nature (London)* **320**, 340 (1986).
- [6] Y. Monovoukas and A. P. Gast, *J. Colloid Interface Sci.* **128**, 533 (1989).
- [7] C. Smits, dissertation, Utrecht, 1991 (unpublished).
- [8] I. S. Sogami and T. Yoshiyama, in Ref. [4], p. 171.
- [9] C. Smits, J. S. van Duijneveldt, J. K. G. Dhont, H. N. W. Lekkerkerker, and W. J. Briels, in Ref. [4], p. 157.
- [10] Y. Monovoukas and A. P. Gast, in Ref. [4], p. 183.
- [11] W. van Meegen, P. N. Pusey, and P. Bartlett, in Ref. [4], p. 207.
- [12] W. Härtl, R. Klemp, and H. Versmold, in Ref. [4], p. 229.
- [13] S. Hachisu, in Ref. [4], p. 243.
- [14] D. J. W. Aastuen, N. A. Clark, L. K. Cotter, and B. J. Ackerson, *Phys. Rev. Lett.* **57**, 1733 (1986); **57**, 2772(E) (1986).
- [15] D. J. W. Aastuen, N. A. Clark, J. C. Swindal, and C. D. Muzny, in Ref. [4], p. 139.
- [16] W. B. Russel, in Ref. [4], p. 127.
- [17] L. Antl, J. W. Goodwin, R. D. Hill, R. H. Ottewill, S. M. Owens, S. Papworth, and J. A. Waters, *Colloids Surf.* **17**, 67 (1986).
- [18] S. E. Paulin and B. J. Ackerson, *Phys. Rev. Lett.* **64**, 2663 (1990).
- [19] B. J. Ackerson and T. A. Morris, *Ceram. Powder Sci.* **3**, 349 (1990).
- [20] W. Weise (private communication).
- [21] B. J. Ackerson, *J. Rheol.* **34**, 553 (1990).
- [22] P. N. Pusey and W. van Meegen, *Ber. Bunsenges. Phys. Chem.* **94**, 225 (1990).
- [23] T. Ohta, D. Jasnow, and K. Kawasaki, *Phys. Rev. Lett.* **49**, 1223 (1982).
- [24] W. I. Goldberg, in *Light Scattering Near Phase Transitions*, edited by H. Z. Cummins and A. P. Levanyuk (North-Holland, Amsterdam, 1983).
- [25] H. Furukawa, *Physica (Amsterdam)* **123A**, 497 (1979).
- [26] M. Avrami, *J. Chem. Phys.* **7**, 1103 (1939); **8**, 212 (1940); **9**, 177 (1941).
- [27] J. W. Christian, *The Theory of Transformation in Metals and Alloys, Part I: Equilibrium and General Kinetic Theory* (Pergamon, New York, 1981).
- [28] I. M. Lifshitz and V. V. Slyozov, *J. Phys. Chem. Solids* **19**, 35 (1965).
- [29] S. M. Allen and J. W. Cahn, *Acta Metall.* **27**, 1085 (1979).
- [30] See, e.g., H. C. Fogedby and O. G. Mouritsen, *Phys. Rev. B* **37**, 5962 (1988); M. C. Tringides, *Phys. Rev. Lett.* **65**, 1372 (1990).
- [31] B. J. Ackerson (unpublished).